Measurement of femtosecond-scale drift and jitter of the delay between the North and South Beams of Gemini

Contact *robert.shalloo@physics.ox.ac.uk*

R. J. Shalloo, C. Arran, G. Cheung, L. Corner, J. Holloway, R. Walczak, S. M. Hooker

John Adams Institute, University of Oxford, Clarendon Laboratory, Parks Road, Oxford, OX1 3PU, U.K.

N. Booth, O. Chekhlov, C. D. Gregory, S. J. Hawkes, C. J. Hooker, B. Parry, Y. Tang

Central Laser Facility, STFC Rutherford Appleton Laboratory, Harwell Campus, Didcot, OX11 0QX, U.K.

Introduction

As the ambition and complexity of high intensity laser plasma experiments increase, the requirements placed on the performance of the laser systems employed for this work become more demanding. Ever stricter bounds are being placed on the laser parameters: pointing stability, energy stability and wavefront quality, to name but a few. For a dual beam system such as Gemini, where two highly energetic ultrashort pulses may be employed at once, there are increasing requirements for high levels of temporal stability between the beams, to allow for accurate and repeatable synchronization of pulse arrival on target. Examples of experimental arrangements requiring a high level of temporal synchronization include staging of laser plasma accelerators [1], external injection techniques [2], Compton scattering [3], Thompson scattering [4] and multi-pulse laser wakefield acceleration [5]. In several of these cases, synchronization to the femtosecond level is required.

In this report we describe an experimental technique for measuring femtosecond-scale drift and jitter in the delay between Gemini's North and South beams. This technique was successfully employed in both an off-shot and on-shot capacity for an f/2-f/40 setup. However, the technique itself could be adapted with little difficulty to other focusing geometries.

The technique for measuring the pulse separation is based on spectral interference. If the North and South beams are separated by a temporal delay Δt, at the entrance slit of a spectrometer, the recorded spectrum will be of the form:

$$\begin{aligned} S(\omega) &= |\; FT[E_{\mathrm{N}}(t) + E_{\mathrm{S}}(t+\Delta\tau)\,]\;|^2 \\ &= \left|\tilde{E}_{\mathrm{N}}(\omega)\right|^2 + \left|\tilde{E}_{\mathrm{S}}(\omega)\right|^2 \\ &\qquad + 2\left|\tilde{E}_{\mathrm{N}}(\omega)\tilde{E}_{\mathrm{S}}(\omega)\right|\cos[\omega\Delta\tau + \phi_{\mathrm{N}}(\omega) - \phi_{\mathrm{S}}(\omega)] \end{aligned}$$

The measured spectrum contains an interference term with a period determined by $\Delta\tau$. Thus, by analysing the fringe spacing of the measured spectrum it is possible to determine pulse separation.

Experimental Arrangement

Figure **1**: Experimental layout for the off-shot timing diagnostic shows the experimental layout for the off-shot implementation of the timing diagnostic on an f/2-f/40 setup, a typical focusing geometry employed on Gemini. For this measurement, a 50.8 mm diameter, 517 mm effective focal length, 15° off axis paraboloid (OAP) was driven into the beamline downstream of the interaction point (IP) to collimate light from the focus. The OAP captured all of the light from the f/40 and an ~8 mm thick annular portion of the f/2 beam. Both beams were then directed out of the chamber using a set of wedges and mirrors, before being telescoped down and focused onto the slit of an Acton SP-2750 imaging spectrometer, which was fitted with an Andor DU940 spectroscopic CCD camera and used a grating of 600 lines per mm.

A fast photodiode inserted at IP allowed for initial gross timing of the two beams to within 50 ps, which is within the measurement range of the spectral interference diagnostic. Once the photodiode was removed, fringes could be observed on the spectrometer, allowing for fine timing of the two beams to the femtosecond level.

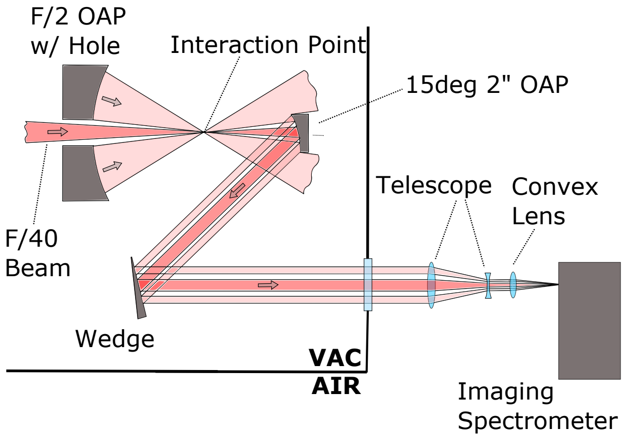

Figure 1: Experimental layout for the off-shot timing diagnostic, located post-IP in TA3.

To allow for measurements of the pulse separation on-shot, a second spectrometer was installed in LA3 on the beam diagnostics table, prior to the pulse compressors. Leaks were taken from behind mirrors in both the North and South beamlines, and these were combined in a beam splitter before being focused onto the slit of the spectrometer. An Acton SP2300i spectrometer was used in conjunction with an Andor DV420 camera and a grating of 600 lines per mm.

This on-shot diagnostic was capable of measuring jitter and drift between Gemini's North and South beams from their splitting point to the two compressors. The off-shot diagnostic, being placed directly post IP, measures the jitter and drift between the beams from the splitting point to IP. Given that the system is under vacuum from the compressors to IP, it would be expected that many of the sources of jitter and drift would occur before the pulse compressors.

Analysis

To find the pulse separation from the fringe spacing, the measured spectrum is first interpolated to a grid which is uniform in frequency rather than in wavelength, and is then Fourier transformed to the time domain. This creates a spectrum of peaks such as shown in Figure **2**b, with a DC peak across the image and clear interference peaks either side of this, where the two pulses are overlapped in space. The time at which these peaks occur indicates the delay between the two pulses, changing the problem into one of peak finding.

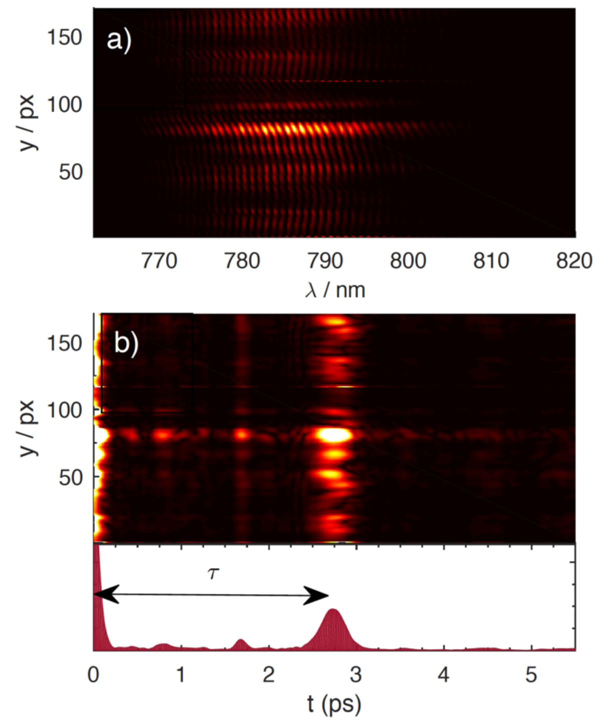

Figure 2: a) An example spectrum showing timing fringes, measured in TA3, from the interference of the North and South Beams separated in time. b) The Fourier transform of this spectrum shows the fringe frequency, which corresponds to a time delay ,$\Delta\boldsymbol{\tau} = (2.74 \pm 0.01)$ ps.

The maximum delay that can be measured, Δt, depends on the choice of diffraction grating used in the spectrometer. This is described by $\Delta t = \frac{\pi}{\delta\omega} \approx \frac{\mathrm{N}\,\lambda_0{}^2}{2c\Delta\lambda}$ for a spectrometer with N pixels and a bandwidth of $\Delta\lambda$. Using more dispersive gratings can reduce the bandwidth and thus increases the maximum time that can be measured, such that with a 1200 lines per mm grating with a bandwidth of $\Delta\lambda = 12$ nm, separations up to $\Delta t = 0.1$ ns can be measured. Figure **3** demonstrates this with results from simulations; the choice of grating controls the delays over which this measurement technique is accurate.

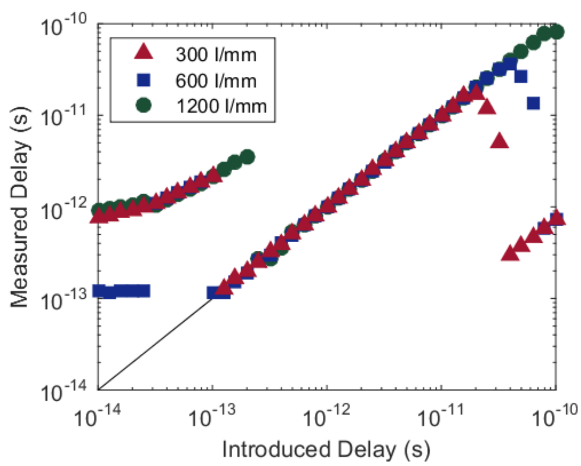

Figure 3: Simulations of measured delay against introduced delay for a range of different dispersions, and hence spectrometer bandwidths. More dispersive gratings are effective at higher delays, up to around 0.1 ns, but fail sooner at small delays of 100s of fs, where the sideband can no longer be resolved from the DC peak.

The resolution, δt, of the diagnostic is also limited by the bandwidth of the spectrometer according to $\delta t = \frac{2\pi}{\Delta\omega} \approx \frac{\lambda_0{}^2}{c\Delta\lambda}$. That is, choosing the least dispersive grating at 600 lines per mm provides a bandwidth of $\Delta\lambda = 57$ nm at $\lambda_0 = 800$ nm, and hence a resolution of $\delta t \approx 37$ fs. Given that the Gemini pulse has a zero to zero bandwidth of approximately 55 nm, the intensity outside the spectrometer bandwidth is close to zero, and so the temporal resolution can be improved with zero-padding without introducing artefacts. Surrounding the original spectrum with zeros such that it is eight times larger increases the resolution to $\delta t \approx 5$ fs. Note that this process is analogous to constructing a bandlimited continuous function by interpolating between the original data points with a sinc function in the Whittaker-Shannon formula [6]. The precision then tends towards a constant value, which is limited by the width of the laser pulse itself, as shown in Figure 4. In practice, noise and real pulse shapes made the precision limit significantly larger than that from simulations.

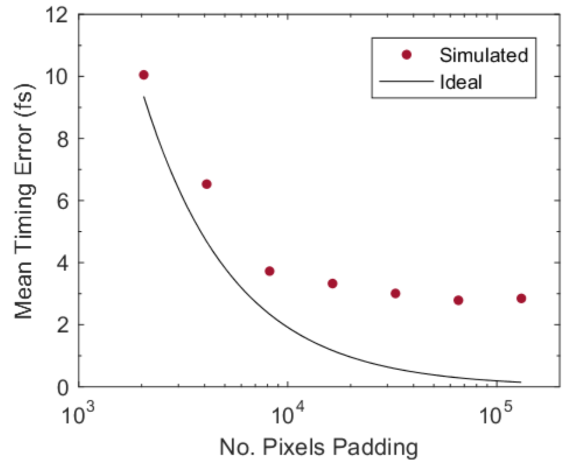

Figure 4: Simulated measurement error against pixels of zero-padding for a 600 lines per mm grating at 800 nm. Increasing the number of points in the frequency grid improves the resolution of the measurement towards zero, but the precision approaches a finite limit.

Results

The off-shot timing measurement, taken post-IP in TA3, was used to measure how the delay between the Gemini North and South beams changed over a long period. Data was recorded for around 80 minutes at midday on June 25th, interrupted by a period in the middle where the spectrometer software crashed. The results are shown in Figure 5. The delay varied significantly, with periodic oscillations on the scale of 100 fs over a period of around 15 minutes. Furthermore, this correlated strongly with a 1°C temperature oscillation in LA3 reported by eCAT [7]. We conclude that even small changes in temperature are sufficient to change the North-South beam timing by 10s of fs, making it difficult to overlap the two beams for more than a few minutes. The exact mechanism by which the temperature variation is causing temporal jitter and drift between the beams is still unclear. We postulate that a combination of temperature gradients within the laser area along with expansion of the steel optical tables could be responsible but further investigation is required.

To investigate where the drift originates and to test the validity of timing measurements made with the on-shot timing spectrometer in LA3 to the pulse timing at IP, both on-shot and off-shot spectrometers were run simultaneously over a period of ~80 minutes at around midnight on July 1st, as shown in Figure 6.

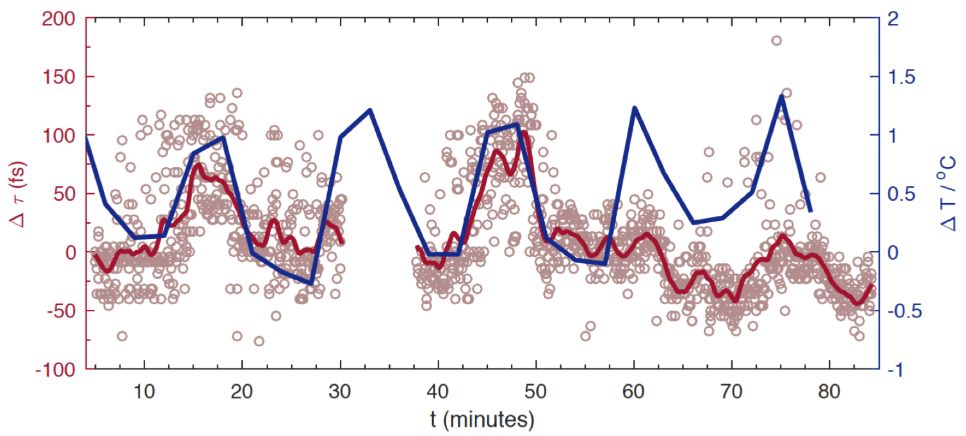

Figure 5: Change in delay between North and South beams measured in TA3 (moving average in red line) against time compared to temperature measured in LA3 (blue line). Variation in delay on the scale of 100 fs correlates strongly with 1 degree changes in temperature which are periodic over around 15 minutes.

Both diagnostics show the same periodic drift in delay, indicating that the source of the variation is located before the LA3 diagnostics table rather than in the target area. This demonstrates that the problem will be common to all experiments in the Gemini area, not particular to any one experimental set up. The TA3 measurement also shows a slower, approximately linear, drift of around 1 fs per minute. The precise source of this drift is unknown but it is thought to occur in the target area, as the distance from the pick off to the LA3 spectrometer was small. A likely candidate for the source of this drift is slow movement with temperature of the Gemini vacuum chamber extension arm although, further investigation is required.

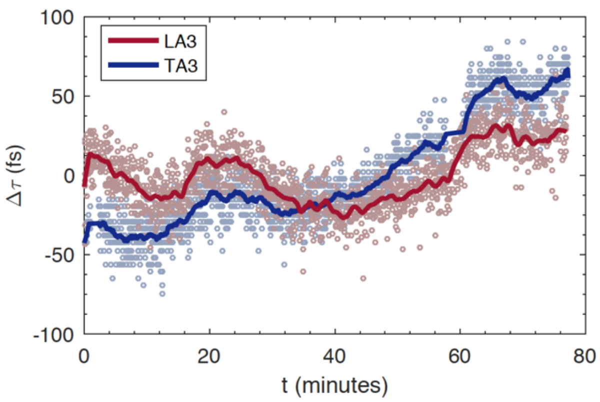

Figure 6: Change in delay between North and South beams measured in both LA3 and TA3 against time. The drifts and oscillations measured by the two diagnostics are strongly correlated, but the TA3 diagnostic experiences an additional slow drift of around 80 fs over 80 minutes.

It is also possible to correlate the LA3 and TA3 measurements shot to shot to understand where the jitter arises. By subtracting the moving averages and plotting only the variations around these, shown in Figure 7, no correlation can be seen, with $\boldsymbol{R^2 = 2.5\times10^{-4}}$. This indicates that the shared contribution to the jitter, with a source before the LA3 diagnostics table, is negligible. The jitters in the LA3 and TA3 measurements are independent and approximately Gaussian distributed with standard deviations of (10.6 ± 0.7) fs and (10.0 ± 0.6) fs respectively. As the measurement error is the same for both spectrometers the contribution to the jitter from the target area is negligible. The only source of the jitter is therefore a measurement error of around (10.3 ± 0.7) fs, which is the precision of the measurement technique.

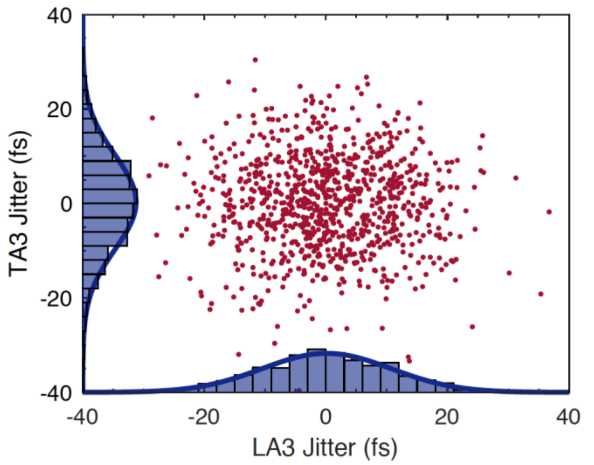

Figure 7: Comparison between jitters from LA3 and TA3 measurements, matched shot to shot. There is no correlation, implying that the jitters are independent random measurement errors with standard deviations of (10.6 ± 0.7) fs and (10.0 ± 0.6) fs respectively.

Conclusions

An accurate method of measuring the time delay between Gemini's North and South Beams to the femtosecond level has been described. This method is based on spectral interference and can be used for different focusing geometries commonly used on Gemini. Using a variety of spectrometer gratings allowed for measurement of pulse delays from under 100 fs up to over 0.1 ns. Zero padding can improve the resolution of this measurement to a few femtoseconds.

The delay between the North and South beams was measured with independent on- and off-shot spectrometers. These show that there is an oscillation of the delay on the scale of 10s of fs over the timescale of 10-20 minutes, which is present before the beams leave the laser area. This oscillation correlates strongly with temperature, and changes in temperature on the scale of 1°C make it difficult to retain overlap between the two beams for longer than a few minutes.

Finally, the shot to shot jitter in the delay between North and South beams was measured to be smaller than the precision of our measurement, (10.3 ± 0.7) fs.

Acknowledgements

Thanks to all the staff at the Gemini facility who made these measurements possible, particularly the on-shot measurement in LA3, which required many days of their time and patience.

References

[1] S. Steinke, J. van Tilborg, C. Benedetti and others, "Multistage Coupling of Independent Laser-Plasma Accelerators," *Nature,* vol. 530, no. 7589, p. 190, 2016.

[2] N. Bourgeois, J. Cowley and S. M. Hooker, "Two-Pulse Ionization Injection into Quasilinear Laser Wakefields," *Physical Review Letters,* vol. 111, no. 15, p. 155004, 2013.

[3] F. Hartemann, D. Gibson, W. Brown and others, "Compton Scattering X-Ray Sources Driven by Laser Wakefield Acceleration," *Physical Review ST AB,* vol. 10, no. 1, p. 011301, 2007.

[4] N. Powers, I. Ghebregziabher, G. Golovin and others, "Quasi-Monoenergetic and Tunable X-Rays from a Laser-Driven Compton Light Source," *Nature Photonics,* vol. 8, no. 1, p. 28, 2013.

[5] S. M. Hooker, R. Bartolini, S. P. Mangles and others, "Multi-pulse Laser Wakefield Acceleration," *Journal of Physics B: At, Mol & Opt. Phys.,* vol. 47, no. 23, p. 234003, 2014.

[6] C. E. Shannon, "Communication in the Presence of Noise," *Proceedings of the IRE,* vol. 37, no. 1, p. 10, 1949.

[7] E. J. Divall, "Laser Performance Data Analysis Tool," *Central Laser Facility Annual Report,* p. 220, 2007/2008.